Using GMI for Intercalibration of the Constellation Sensors

T. Wilheit
Department of Atmospheric Science, Texas A&M University
Hendersonville, NC

Note: All of the analyses presented here are based on matchup data sets produced by the Remote Sensing Laboratory of the University of Central Florida

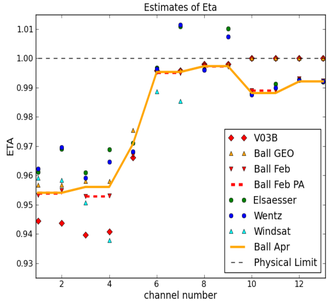

Comparisons with Windsat
Double Differences (G-W)

10V	10H	18V	18H	23V	37V	37H	RMS
V03B							
2.84	1.54	2.73	0.03	-0.00	**-1.52**	**-1.56**	1.80
Geometric Optics							
0.68	0.32	-0.95	-2.18	-2.11	**-1.54**	**-1.58**	1.49
Ball Feb							
1.29	0.49	0.08	-1.53	-0.22	**-1.40**	**-1.43**	1.09
Ball Feb Pol Averaged							
1.14	0.57	0.07	-1.52	-0.22	**-1.36**	**-1.45**	1.07
Ball April							
1.14	0.57	-0.55	-1.92	-1.06	**-1.40**	**-1.48**	1.25

Comparisons with MetOpB
Double Differences (G-M)

89V	89H	166V	166H	±3	±7	RMS
V03B						
0.07	1.07	-3.21	-2.96	**-2.18**	**-2.51**	2.28
Geometric Optics						
0.21	1.11	-3.17	-2.93	**-2.24**	**-2.52**	2.28
Ball February						
-0.29	1.06	-0.37	-0.07	**0.06**	**-0.44**	0.51
Ball February Pol Averaged						
-0.26	1.04	-0.36	-0.08	**0.06**	**-0.44**	0.50
Ball April						
-0.22	1.04	-0.10	0.18	**0.30**	**-0.34**	0.48

Going the Other Way (M-G)

89	157	±1	±3	190.	RMS
0.38	**-0.47**	0.05	**-0.35**	**0.22**	0.33

Search for the "Perfect" Calibration

Figures Above

It was clear early on that the original calibration of GMI (V03B) wasn't very good. Comparison with sensors thought reliable (*e.g.* Windsat and the MetOps) as well as with model calculations yielded unreasonable discrepancies. The source of the calibration errors appears to be the fraction (η) of the total antenna pattern that intersects the Earth in normal observations. Originally, the instrument manufacturer, Ball Aerospace, had estimated η using antenna pattern models. The calibration book and, as a consequence, the V03B calibration were based on a physical optics model for frequencies below 100 GHz. Above that they provided no estimate so an η value of 1 was used. [Red diamonds in the figure] One is the physical limit of a perfect antenna of infinite size. They also used a geometric optics model for the same frequenciesb but they considered the physical optics model to be the better of the two.

We used several other approaches. We calculated the η values from GDAS based single-differences but with a water vapor profile retrieved from MetOpB-MHS. This was done using both the Elasesser and the Wentz surface model. We also used Windsat-GMI double differences (Wentz-based) for the η values. The GDAS-based approaches led to unphysical values at 36H and 89H.

Ball first reported their analysis of the satellite attitude maneuvers in February and recommended using the new values for the 166 and 183 GHz. It was clear that these new Ball values were much closer to reality than were the V03B values which where patently unphysical. It was also noticed that the new η values at lower frequencies also seemed more reasonable. In order to satisfy the constraint from the nadir viewing maneuver, the two η values at each polarization should be averaged. The comparisons with Windsat were very good with the Feb. Ball values and very slightly better when averaged by polarization (PA). By April, Ball had fine-tuned their analysis and had developed an error model. The April values have the most defensible physical basis and have been accepted as the official calibration for GMI (and by extension) the entire constellation even though their comparison with Windsat is somewhat worse. **The prelaunch values were based on antenna pattern modeling and the current values are based on observations. Selecting on the basis of comparisons with other satellites would not have been honest.**

TMI – GMI Double Differences

GDAS 22674 Samples

	10V	10H	19V	19H	23V	37V	37H	85V	85H
DDs	-2.34	-1.99	0.48	-0.17	-0.31	-1.92	-1.02	-1.04	-1.24
@	171.	89.	203.	138.	225.	216.	156.	264.	233.

Classic Fit 15806 Samples

DDs	-2.29	-2.00	0.34	-0.50	-0.35	-1.86	-0.98	-0.91	-1.11
@	170.	89.	200.	133.	220.	214.	152.	261.	228.

Water Vapor Profile Fit 13006 Samples

DDs	-2.34	-1.97	0.20	-0.62	-0.50	-1.92	-1.02	-1.06	-1.21
@	172.	90.	207.	145.	232.	219.	161.	267.	242.

Improved Fit 11218 Samples

DDs	-2.29	-1.97	0.42	-0.25	-0.49	-1.86	-1.00	-1.04	-1.29
@	172.	91.	208.	147.	234.	220.	163.	269.	245.

The 4 algorithms described below have been applied to the TMI-GMI pair (among others). The DDs in the table above show the consistency of the various methods. Below 100 GHz we consider the "Improved Fit" to be the most reliable and above 100 GHz the "Water Vapor Fit" Although the Improved Fit is nominally to be preferred for the 85 GHz channels, it's really pretty much of a toss-up with the Water Vapor Fit. Even for the Algorithm/Frequency pairs such as the WV Fit with the 10-37 GHz channels for which we wouldn't expect great performance, the results do not differ much from the other algorithms. The degree of consistency observed here gives us great confidence in the results.

It's also worth noting the absolute values of the TMI-GMI DDs; they are generally not small. Since we now have great confidence in the absolute calibration of GMI (<1K RMS for these channels), we must conclude that the absolute calibration of TMI is rather poor. Although it is not shown here, comparisons with TMI and Windsat have indicated that TMI is extremely stable making it suitable for a transfer standard even if not an absolute standard.

The figure above right gives a glimpse of that stability. Here we have plotted the TMI-GMI DD anomaly month-by-month for the full TMI-GMI overlap period. Even with the descent of TRMM from 405 Km to 335 Km, there is no secular drift visible in these plots. In its last days, TMI was quite stable, and our corrections for changing Earth Incidence Angle worked well.

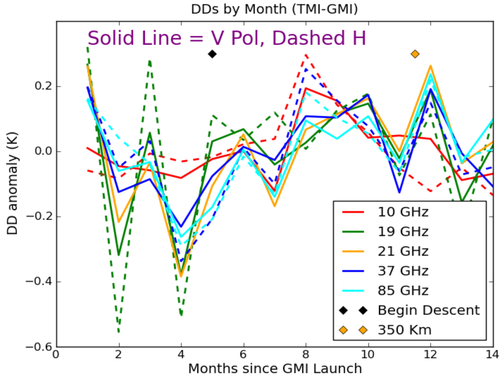

Comparison of Metop and NOAA MHSs (MHS- GMI DDs)

89	157	±1	±3	190.	RMS
METOPA	14317 Samples				
0.44	-0.41	0.16	-0.32	0.33	0.35
METOPB	18981 Samples				
0.38	-0.47	0.05	-0.35	0.22	0.33
NOAA18	16123 Samples				
-0.08	-0.48	0.26	-0.02	0.23	0.27
NOAA19	21303 Samples				
-0.04	-0.23	0.52	0.11	0.22	0.28

@	256.	284.	248.	262.	272.

Here we show the DDs for all the presently functioning MHSs. They are all quite small and, for the most part, even closer to one another.

EIA Dependence of Cross-Track Scanners

Figures Right and Below

The Earth Incidence Angle (EIA) of GMI is approximately constant at a little over 50° depending on channel. On the other hand, cross-track scanners such as SAPHIR, MHS and ATMS have EIAs that vary from 0° (*i.e.* Nadir) to greater than 60°. Intercalibration algorithms must handle these EIA differences. How well they handle the angles provides insight into the performance of the algorithms.

We have applied 4 different algorithms to various sensors in the constellation; here we concentrate on the cross-track scanners. The simplest algorithm (termed "GDAS" in the figures) is to take a data base such as the GDAS analysis product co-located with the observations of both sensors and use it to compute expected brightness temperatures which are then used to compute the desired Double Differences. Another algorithm Uses the temperature profile, surface temperature and windspeed from GDAS to retrieve a water vapor profile by fitting to the 6 highest frequency channels of GMI. This retrieved WV profile is substituted for the GDAS WV profile in the above method.(termed "WV Fit" in the figures). For the channels above 100 GHz this is the preferred algorithm.

For the imager channels, we use the radiances below 100 GHz to retrieve the cloud liquid water, water vapor, sea surface temperature and sea surface wind speed with a fixed relative humidity profile. The temperature profile is adjusted as a proxy for the water vapor profile. This algorithm has been in use for some time so it is termed "Classic" in the figures. Finally the RH and temperature profiles from the WV fit are substituted into the Classic fit for an "Improved" fit. The improved fit is preferred below 50 GHz. For the channels in the 80-100 GHz range the Improved and WV fit have similar reliability. As an example, the results from all 4 algorithms applied to GMI-TMI matchups are shown above-right.

In the first 5 figures we show the DDs between the MHS on MetOpB and GMI for all 5 MHS channels as a function of MHS Earth Incidence Angle. The calculations were performed using both the Elsaesser and Wentz surface emissivity models. We consider a P-P variation of 0.5K of the DDs acceptable. (It will look more-or-less like NEΔT to the precipitation retrievals.) In every case it can be seen that the EIA dependence is less with the Wentz surface emissivity model than with the Elsaesser model, significantly so in some cases. If we use the Wentz surface model, then the EIA dependence of all 5 MHS channels is acceptable. The 183 ±1 GHz channel might be expected to be problematic because the GMI does not have a similar channel, but by this test, the DDs are quite stable. Similar results were observed for the MHSs on MetOpA, NOAA 18 and NOAA 19. We also show the EIA dependence for several SAPHIR channels. Here the performance is quite good, even for the ±0.2 GHz channel.

However not everything is sweetness and light. For several channels of ATMS we have significant problems. The pattern for the 23 and 31 GHz channels suggests some beam blockage at the edges of the scan. It appears that some high emissivity material intercepts part of the beam near both edges of the scan. We recommend that these channels not be used beyond an |EIA| of 40°. The 88GHz channel has a different problem. The "W" shape suggests that the feed horn is not perfectly linearly polarized but rather has a circular polarization component. The slope suggests that the linearly polarized component is rotated slightly towards the high numbered scan positions. The last figure shows the original ATMS EIA dependence and with the assumption of 20% (power) in circular polarization and a 1° rotation of the linear component. For comparison the MHS EIA dependence of the corresponding channel is shown.